6th Symposium on Launcher Technologies, November 8th to11th, 2005, Munich

# Resonance Frequencies and Damping in Combustion Chambers with Quarter Wave Cavities

Zoltán FARAGÓ
Michael OSCHWALD
Institute of Space Propulsion, DLR Lampoldshausen, D 74239 Hardthausen, GERMANY
zoltan.farago@dlr.de

**Abstract –** In the present study, the eigenmodes of a cylindrical chamber without and with coupling to an absorber cavity are taken under examination. The spectrum of eigenmodes is determined and the damping of modes is characterized by the line-width of the resonances. It is found that usually damping for a given acoustical eigenmode is connected to an increase of the intensity of another one. For the acoustically coupled system of a cylindrical resonator and an absorber cavity it is shown that the eigenfrequencies and other properties of the acoustical eigenmodes deviate from those of the uncoupled cylindrical resonator. The damping is investigated as a function of resonator length and the optimal length for efficient damping is discussed. The damping can be increased by the application of capillary volume at the rear end of the absorber.

## 1 – Theoretical background

In rocket engines, undesirable oscillation of combustion is usually caused by tangential modes. At the Institute of Space Propulsion, in DLR Lampoldshausen acoustical experiments are carried out using common research chambers for both, hot fire [1] and cold flow tests. The experiments presented in this work do not involve combustion or injection; rather they use a model combustion chamber filled with air at room temperature to allow easier and more fundamental characterization of the acoustic processes at work,

In the present study, the abbreviation for the axial, radial and tangential modes is L, R and T, respectively. The number before the abbreviation enables the mode identification. Exemplarily, 1L means the axial or length basic tone, 2L the first axial harmonic, 3L the second axial harmonic, and so on.

The oscillation frequency for the length mode of a half wave tube (a tube with two open or two closed ends) can be predicted as

$$f_l = \frac{l \cdot c}{2 \cdot L} \qquad (l = 1, 2, 3 \ldots) \tag{1}$$

with $f$ (Hz) as the frequency, $c$ (m/s) as the speed of the sound, $L$ (m) as the tube length and $l$ as the mode number. The frequency of the resonance in axial direction in a quarter wave tube (a tube with one open and one closed end) is

$$f_l = \frac{(2 \cdot l - 1) \cdot c}{4 \cdot L} \qquad (l = 1, 2, 3 \ldots). \tag{2}$$

The frequency of transverse modes in cylindrical chamber can be calculated as

$$f_{m,n} = \frac{\alpha_{n,m} \cdot c}{2 \cdot \pi \cdot r} \qquad (m = 1, 2, 3\ldots \text{ and } n = 0, 1, 2\ldots) \tag{3}$$

with $\alpha_{n,m}$ as the eigenvalues of the Bessel function, *m-1* and *n* being the mode numbers of radial and tangential oscillation. The radius of the chamber is *r*. The axial-transverse-combination-frequency is

$$f_{l,m,n} = \sqrt{f_l^2 + f_{n,m}^2} \tag{4}$$

with *l, m, n* as the order of the L, R and T modes.

The spectral energy density or intensity of the different modes can be predicted from the definition of the unit decibel as

$$\mathrm{dB} = 10 \cdot \log(I_1/I_2) \tag{5}$$

with $I_1$ and $I_2$ as the spectral energy density of the oscillation of the eigenmodes 1 and 2.

## 2 – The experimental procedure

The experimental rig is exhibited in figure 1. The dimensions of the cylindrical chambers and resonators are shown in table 1.

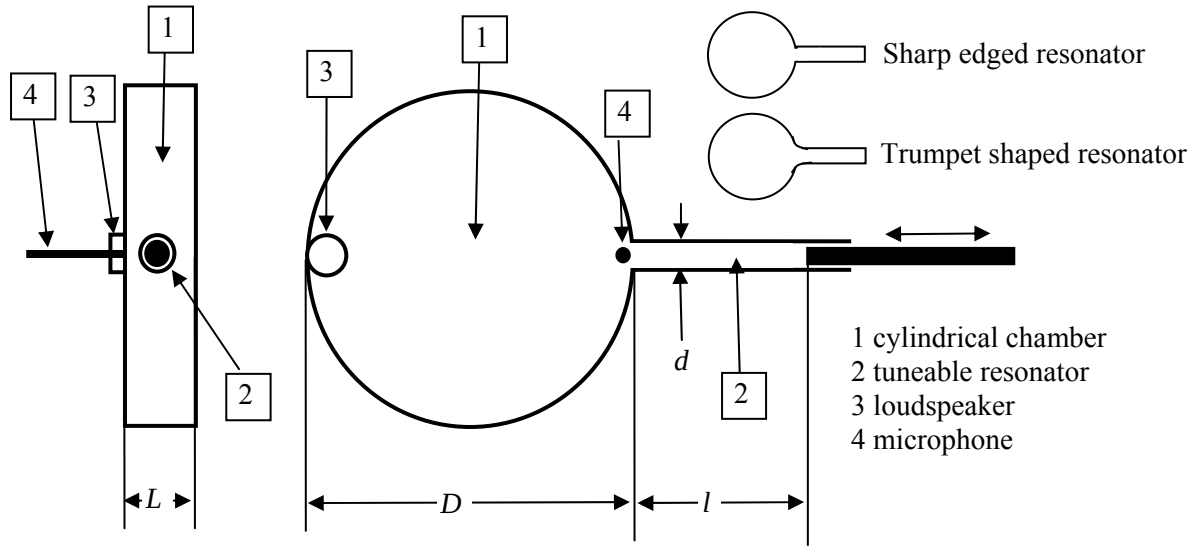


FIGURE 1: Sketch of the experimental device

| Chamber No. | Chamber | | Cavity | | |
|---|---|---|---|---|---|
| | Diameter *D* | Length *L* | Number | Diameter *d* | Length *l* |
| 1 | 200 | 42 | 1 | 12.3 and 10 | 0 to 180 |
| 2 | 220 | 44 | 42 | 9 | 0 to 90 |

TABLE 1: Dimensions of the experimental device

While exciting the cylindrical chamber, the microphone voltage signal shows the pressure oscillation. The fast Fourier transform (FFT) analysis of the microphone signal exhibits the frequency distribution. The chamber is excited by a loudspeaker. For excitation a Visaton K 50 WP 50 Ohm full range speaker was used with a frequency response of 180 – 17000 Hz and a response frequency of 300 Hz. The sound signal is measured by a Microtech Gefell measuring microphone MV 302. For acoustical analysis the common software HobbyBox® 5.1 has been used. The single sinusoidal signal was generated by the function generator Yokogawa FG 220, the MLS signal, a kind of repeatable white noise sequence, by HobbyBox® itself.

The identification of the modes is carried out by comparison of the frequency distribution of the measured signal to the predicted mode frequencies. Table 2 shows the mode identification for the experiments with chamber No. 2 for $c$ = 345 m/s.

| No. | n | m | $\alpha_{nm}$ | Mode | Calculated frequency (Hz) | Measured frequency (Hz) | Relative energy density Imax = 100% | Intensity distribution Σ =100 % |
|---|---|---|---|---|---|---|---|---|
| 1 | 1 | 1 | 1.8410 | 1T | 919 | 930 | 100 | 41.6 |
| 2 | 2 | 1 | 3.0541 | 2T | 1525 | 1530 | 50 | 20.8 |
| 3 | 0 | 2 | 3.8318 | 1R | 1913 | 1910 | 20 | 8.3 |
| 4 | 3 | 1 | 4.2013 | 3T | 2097 | 2100 | 40 | 16.6 |
| 5 | 4 | 1 | 5.3175 | 4T | 2654 | 2660 | 16 | 6.7 |
| 6 | 1 | 2 | 5.3320 | 1R1T | 2661 | 2670 | 4.5 | 1.7 |
| 7 | 5 | 1 | 6.4160 | 5T | 3203 | 3210 | 5 | 2.1 |
| 8 | 2 | 2 | 6.7085 | 1R2T | 3349 | 3350 | 2.5 | 0.9 |
| 9 | 0 | 3 | 7.0155 | 2R | 3502 | 3500 | 0.25 | <0.1 |
| 10 | 6 | 1 | 7.5018 | 6T | 3745 | 3740 | 0.3 | 0.1 |
| 11 | - | - | - | 1L | 3920 | 3910 | 0.1 | <0.1 |
| - | 3 | 2 | 8.0146 | 1R3T | 4001 | not found | - | - |
| 12 | - | - | - | 1L1T | 4026 | 4010 | 1.6 | 0.4 |
| 13 | - | - | - | 1L2T | 4206 | 4200 | 1.3 | 0.25 |
| - | 1 | 3 | 8.5363 | 2R1T | 4261 | very weak | - | - |
| - | 7 | 1 | 8.5781 | 7T | 4282 | not found | - | - |
| - | - | - | - | 1L1R | 4362 | very weak | - | - |
| 14 | - | - | - | 1L3T | 4446 | 4430 | 1.3 | 0.25 |
| 15 | 4 | 2 | 9.2825 | 1R4T | 4634 | 4620 | <0.1 | <0.1 |
| 16 | | | - | 1L4T | 4734 | 4720 | <0.1 | <0.1 |
| 17 | 8 | 1 | 9.6475 | 8T | 4816 | 4820 | <0.1 | <0.1 |

TABLE 2: Acoustical modes presented in figure 3; speed of sound $c$ = 345m/s

The measuring procedure contains two steps: 1) The chamber is acoustically excited by a white noise. This step permits to determine at least the first 20 acoustical modes. However, the signal quality of this method is weak and the result is useable for frequency determination only. 2) The acoustical mode in question is excited a second time by its eigenfrequency. This step results in a high quality signal which enables the determination of all acoustical quantities. The duration of the single sinus signal was 50 ms, the output level was 2V. Figure 2 demonstrates the raw signal of the first tangential mode excited by its eigenfrequency. Origin of the FFT analysis is the sudden interruption of the excitation signal.

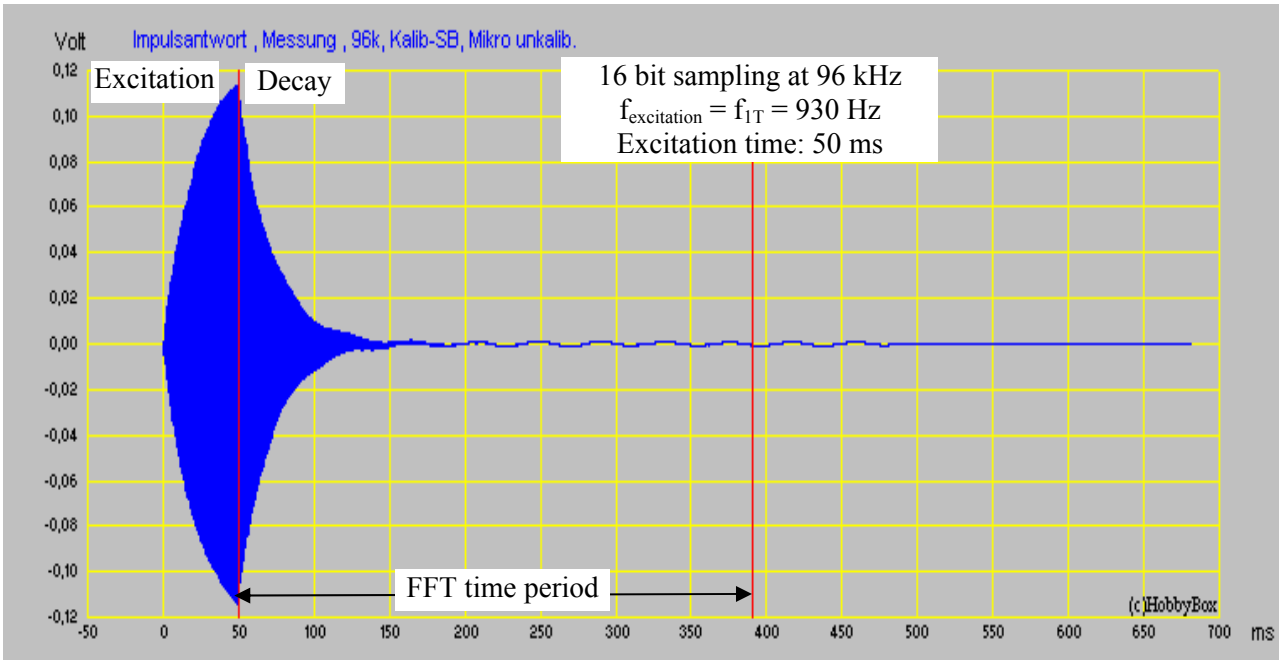


FIGURE 2: Signal of excitation and decay of the 1T mode
Chamber No. 2; cylindrical chamber without cavity

## 3 – Hierarchy of acoustical modes in a cylindrical chamber

Acoustical modes can be excited by different acoustical signals, among others by white noise or by a single sinusoidal signal. The sinus signal may have the eigenfrequency of the mode to be excited, but it can also be a signal having a different frequency. According to linear acoustics there is no energy exchange between different acoustical modes. Our results show, however, that linear acoustic theory cannot explain all features we have found in our experiments. We observe energy transfer between modes, a phenomenon, which is beyond linear theory. The goal of the following experiments is the determination of the eigenfrequencies of the combustor coupled with quarter wave tubes and to investigate the mode conversion process.

The experiment presented in figure 3 shows the FFT-result of the pressure oscillation in the frequency range of 800 to 5000 Hz using white noise excitation. In this frequency range different basic tints, as the first tangential, the first radial and the first axial modes, can be seen including their overtones. Table 2 contains the first 21 tones being presented in figure 3. In table 2 are, however, only 17 tones numbered, since four overtones indicate only very weak signal. The 1T mode (mode No. 1 in table 2) has the highest intensity among all acoustical modes, followed by the second (No. 2) and the third tangential ones (No. 4) which show an intensity of about 50 and 40 % of the 1T mode, respectively. The first three tangential modes are followed by the 1R (No. 3) and 4T (No. 5) modes having a relative intensity of 20 and 16 % compared to the 1T mode, respectively. The sixth place in the ranking possesses the 5T mode (No. 7) with a relative amplitude of about 5 % followed by the 1R1T (No. 6) and 1R2T (No. 8) combination modes with a relative intensity of about 4 and 2.5 %, respectively. The energy density of the 1L1T (No. 12), 1L2T (No. 13) and 1L3T (No. 14) modes is just above the 1% level of the 1T mode. The term "pedestal intensity" is explained in figure 3. The Full Width of Half Maximum (FWHM, see figure 4) of a mode is overestimated for pedestal intensities below 10 dB and strongly overestimated for values below 5 dB.

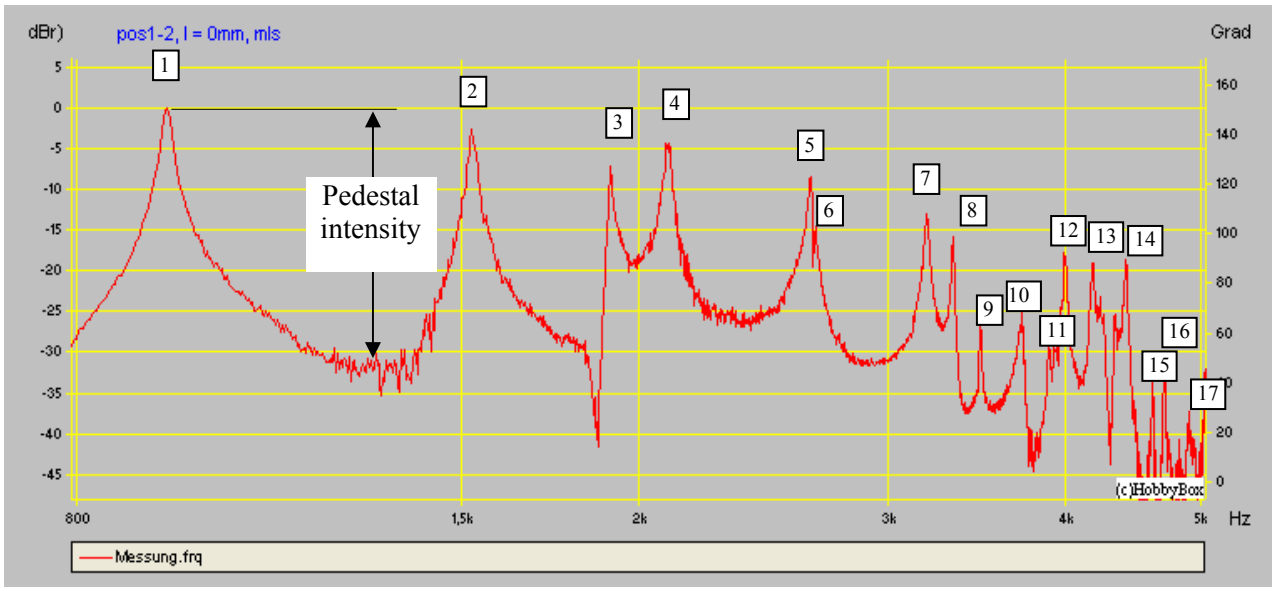


FIGURE 3: Frequency distribution at white noise excitation

Figures 2 – 9 present experiments with chamber No. 2 without cavity. The mode identification numbers on these figures refer to table 2.

Figures 4 to 6 show the frequency distribution for excitation of different eigenmodes by their eigenfrequencies. As can be seen, the relative energy density of the excited modes decreases with increasing excitation frequency. Figure 4 presents the frequency distribution of the 1T mode excited by its eigenfrequency. As can be observed, the intensity of the 1T mode is over 35 dB higher than that of the following 2T mode. This means that the intensity of the 2T mode (No. 2) is less than 0.03 % of the 1T mode's intensity. Figure 5 presents the frequency distribution for the 5T mode excitation (No. 7). The experiment in figure 6 shows the frequency distribution of the 8T mode excitation (No. 17). The difference intensity, as shown in figure 5, enables to predict the relative energy density of a mode using equation (5). The energy density then is the basis for the calculation of the intensity distribution as presented in table 2.

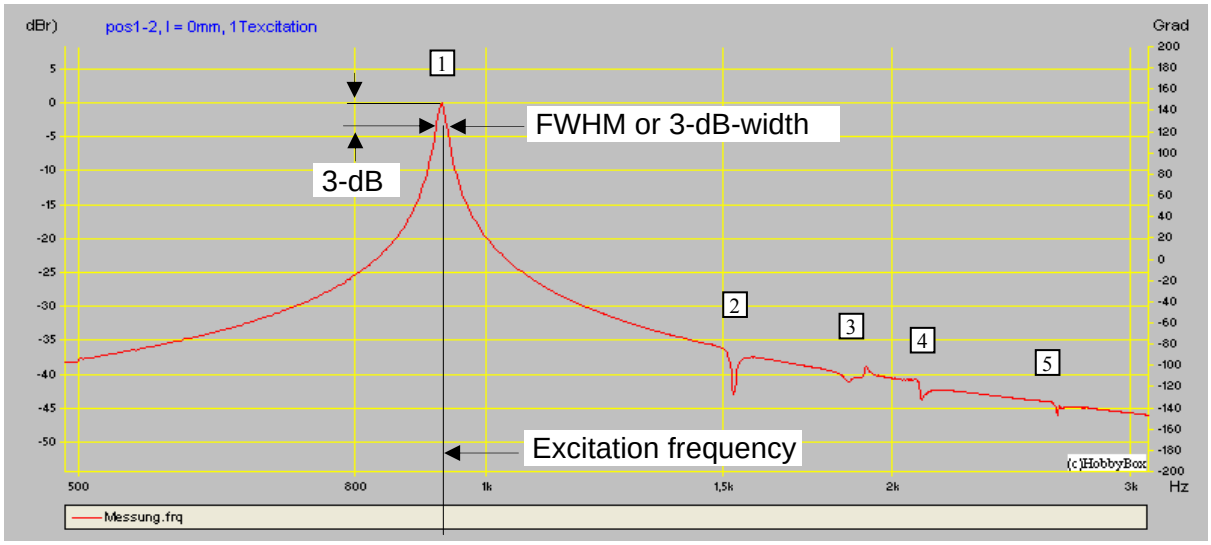


FIGURE 4: Frequency distribution at excitation with 1T eigenfrequency (No. 1, 930 Hz)

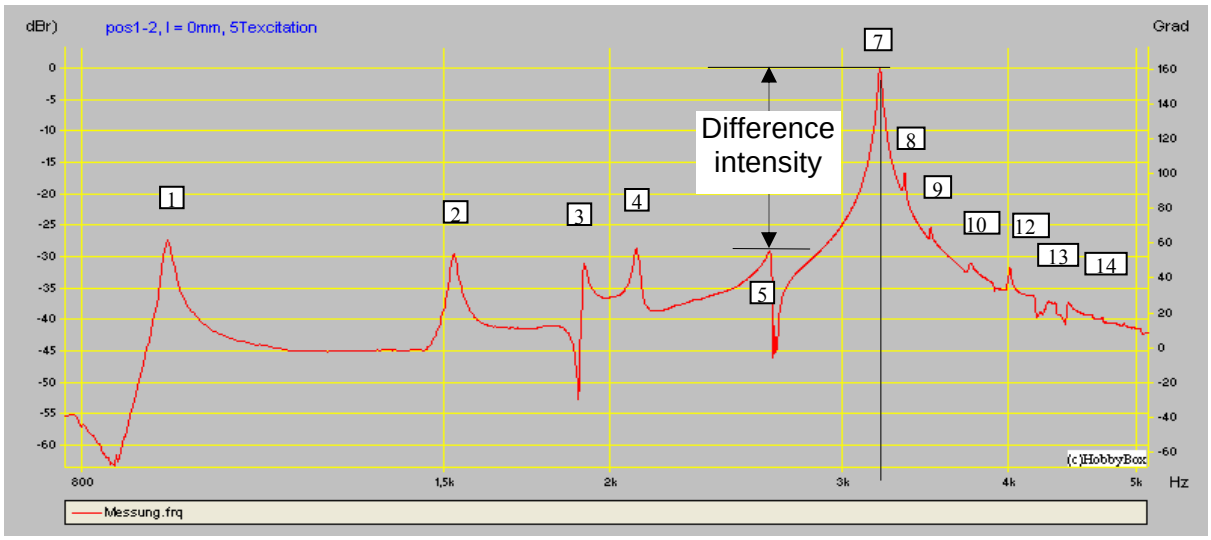


FIGURE 5: Frequency distribution at excitation with 5T eigenfrequency (No. 7, 3210 Hz)

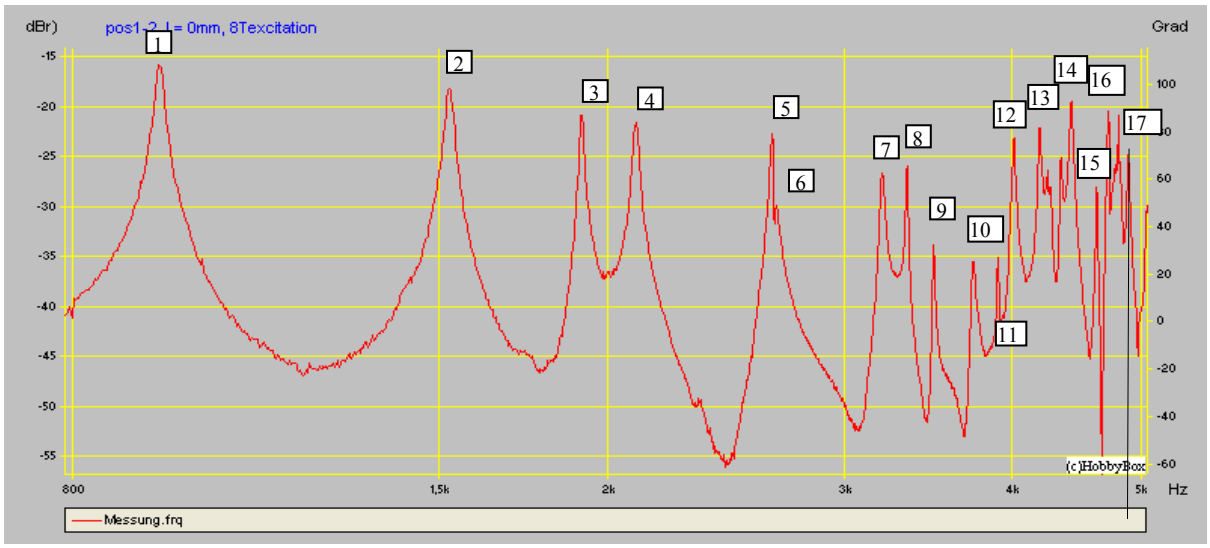


FIGURE 6: Frequency distribution at excitation with 8T eigenfrequency (No. 17, 4820 Hz)

Looking to figure 6 it can be seen that the excitation of the 8T mode (No. 17) by its eigenfrequency excites all lower eigenmodes. The excitation of the lower order modes in figure 6 is even of higher quality than the white noise excitation presented in figure 3. Thus, the energy of the 8T eigenmode converts into all other lower order acoustical eigenmodes.

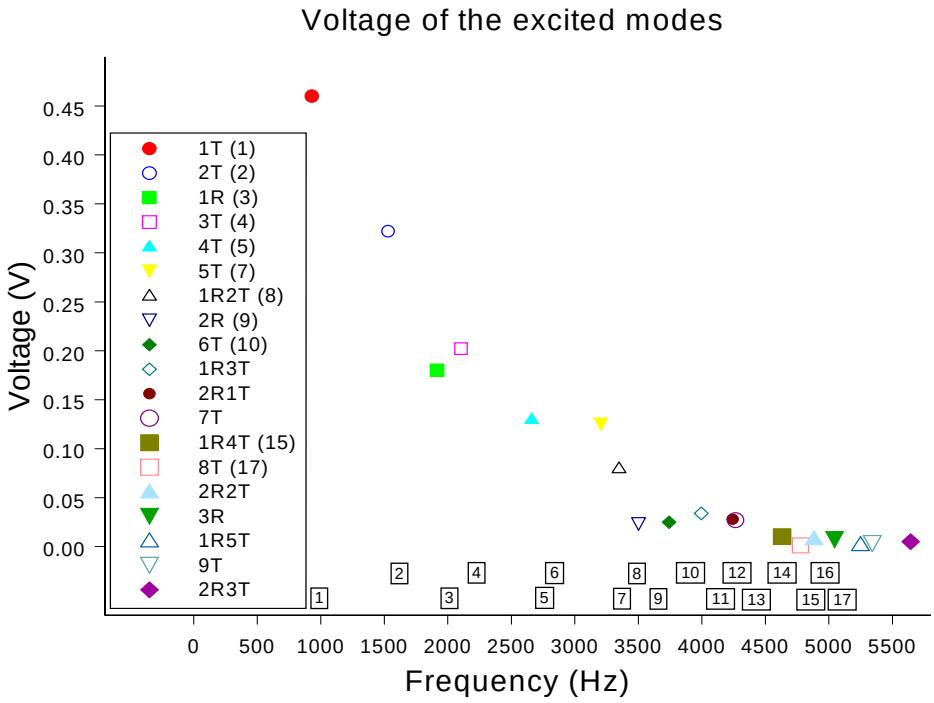


FIGURE 7: Microphone voltage of the acoustical modes excited by their eigenfrequencies

Figure 7 demonstrates that the microphone voltage decreases with increasing excitation frequency. This experimental finding can be explained by the fact that the high frequency excitation energizes many modes rather than excitation at lower frequencies. Since the oscillation of the multiplicity of the excited modes is not synchronized, the pressure peak is lower than that of an excitation by lower frequencies.

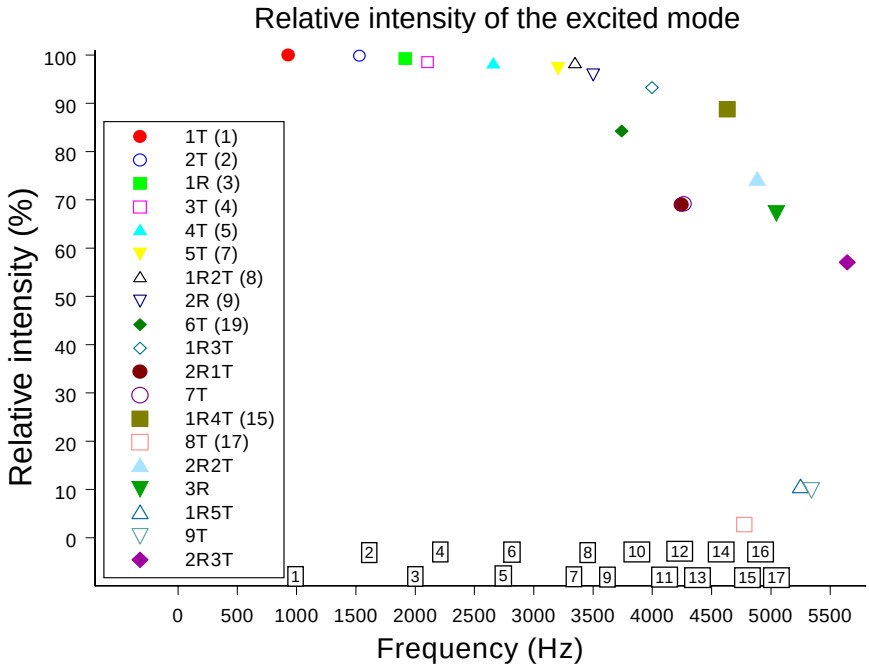


FIGURE 8: Intensity of the acoustical modes excited by their eigenfrequencies

Figure 8 presents the decrease of the intensity of the excited modes with increasing excitation frequency, while 100 % is the sum of all intensities. This experimental result is an evidence of the energy conversion from higher order into lower order modes.

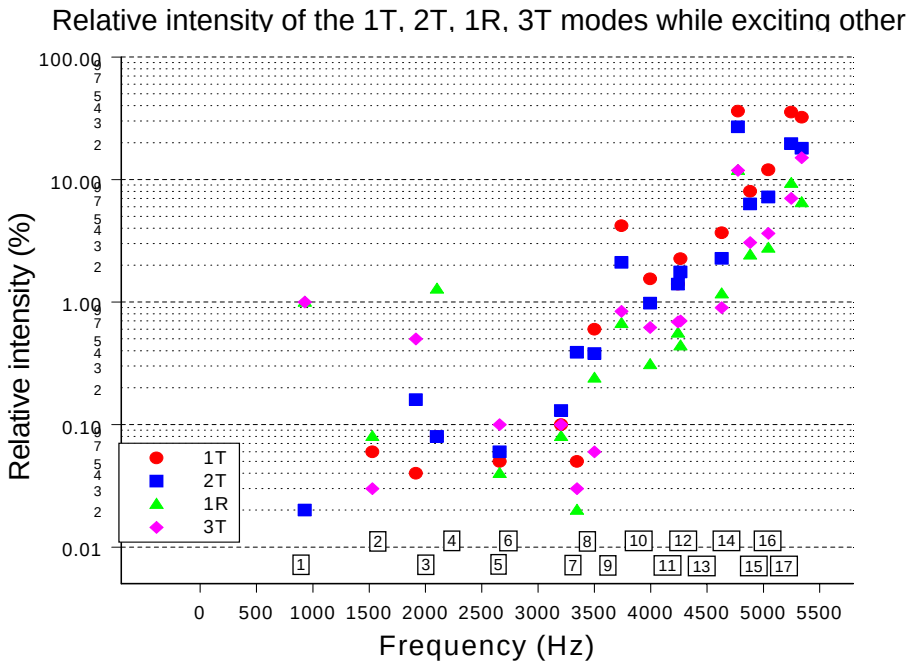


FIGURE 9: Intensity of the 1T, 2T, 1R and 3T modes while exciting other modes

Figure 9 exposes very strong evidence for the mode to mode conversion and for the hierarchy of acoustical modes. The intensity of the 1T, 2T, 1R and 3T modes is plotted VERSUS the excitation frequency. The plotted modes are not excited by their eigenfrequencies but by the frequency of other modes. It can be observed that the intensity of the non-excited modes increases with increasing excitation frequency: Thus, the incoming energy into the non-excited eigenmodes increases with increasing excitation frequency. Furthermore, we obtain the hierarchy of the acoustical modes for a cylinder without quarter wave cavities: The highest intensity has the first tangential mode, followed by the second and the third tangential modes. Thus, higher order modes are emitting energy to lower order ones. The higher the eigenfrequency of the emitting mode, the higher will be the amount of the emitted energy. The lower the eigenfrequency of the receiving mode, the higher will be the received energy amount.

## 4 – Hierarchy of acoustical modes in a cylinder coupled with a quarter wave cavity

In the experiment presented in figure 10, the chamber was excited by the eigenfrequency of the coupled system. The coupled frequency changes stepwise with the increasing resonator length as can be observed in figure 10. *First step:* For low resonator length the frequency decreases very slowly with increasing resonator length: The system frequency seems to cling to the calculated cylinder eigenfrequency. *Second step:* When the resonator length gets close to a value at which the eigenfrequency of the coupled system converges to the calculated λ/4-requency, the system eigenfrequency seems to cling to the calculated frequency of the λ/4-tube. *Third step*: The coupled system eigenfrequency begins to converge to the value of a lower cylindrical mode. This phenomenon was first described by Searby et al. [2].

If the resonator length is leading to a λ/2-tube-frequency which equals a cylinder frequency of the chamber, thus, if equations (1) and (3) are leading to the same value, the acoustical properties of the given eigenmode of the coupled cylinder-resonator-system are equal to the proper eigenmode properties of the cylinder without resonator. In figure 10, the dotted line crosses the measured frequencies of the coupled system. Exemplary, $f_{2T,\,L=0} = f_{1R,\,L=105}$ means that all acoustical properties of the 1R mode at L = 105 mm are identical to those of the 2T mode at L = 0.

If the λ/4-tube-frequenc of the resonator is equal to the coupled frequency of the chamber-resonator-system, the experiment shows very low amplitude and high damping. In figure 10, the dash line crosses the measured frequencies. The damping, in these cases, is affected by the mode to mode conversion.

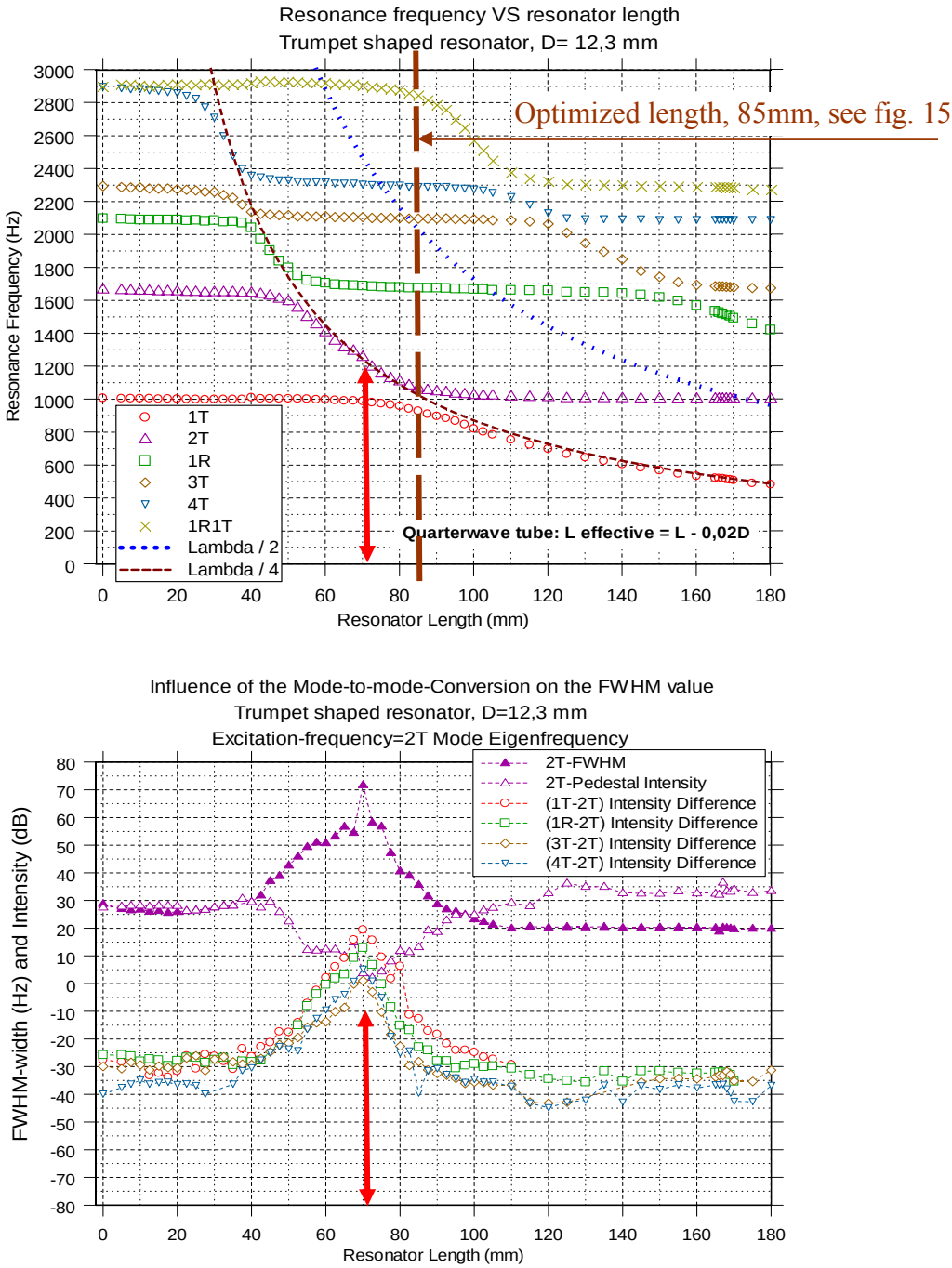


FIGURE 10 (upper plot): Coupled frequency of the chamber-resonator-system
FIGURE 11 (lower plot): Acoustical properties of the coupled system, $f_{excitation} = f_{2T}$
Chamber No. 1, trumpet shaped resonator, resonator diameter D = 12.3 mm

At 72 mm resonator length, the following events can be observed from figures 10 and 11: The 2T mode resonance frequency of the coupled system equals the λ/4-frequency of the resonator (figure 10). The FWHM of the 2T mode has a maximum (solid triangle, fig. 11). The pedestal intensity (see figure 3) becomes a minimum (empty triangle, figure 11). Caused by the very low pedestal intensity, the measured FWHM-width of the 2T mode might be overestimated. In the resonator length range of roughly 60 to 80 mm a half-maximum-width of about 50 Hz seems to be more realistic. The intensity of the 1T frequency has a maximum at +20 dB (empty circle, figure 11): This means that the spectral energy density of the non-excited 1Tσ mode is about 100 times higher than that of the excited 2T. The intensity of the 1R frequency has a maximum at +13 dB (empty square, figure 11): Thus, the intensity of the non-excited 1R mode is about 20 times higher than that of the excited 2T.

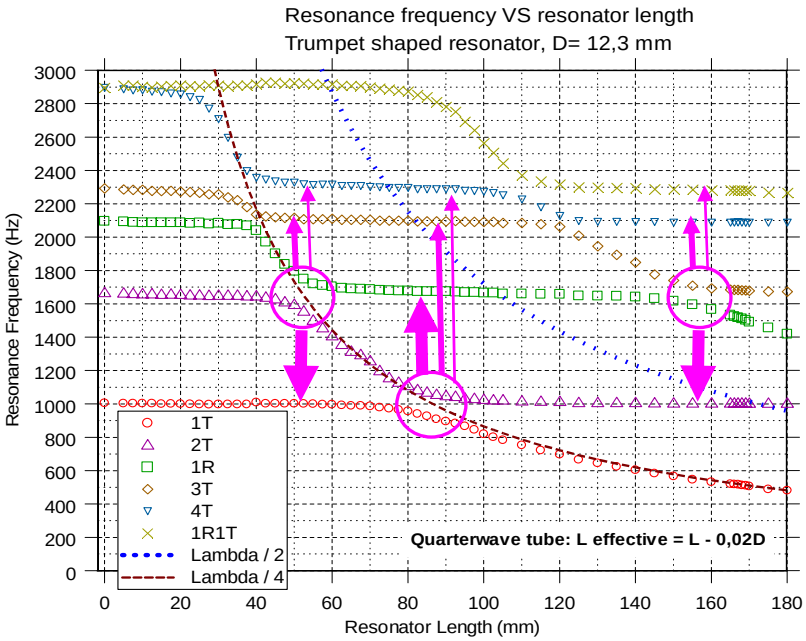


FIGURE 12: Mode conversion map; chamber No. 1, trumpet shaped resonator, D = 12.3 mm

Figure 12 presents the areas at which the coupled resonator prevents pressure oscillation for the 1T and 2T modes via mode conversion. The arrows show the direction of energy movement. The thickness of the arrows indicates the energy flux.

## 5 – Increasing the acoustical damping of a chamber coupled with a quarter wave cavity

Several experiments have been carried out to understand the influence of the cavity shape on the acoustical damping. The goal is to find geometry constellations with high acoustical damping to prevent high frequency combustion oscillation. Figure 13 shows results of measured FWHM distribution for the first and second tangential mode of a sharp edged and a trumpet shaped resonator as shown in figure 1.

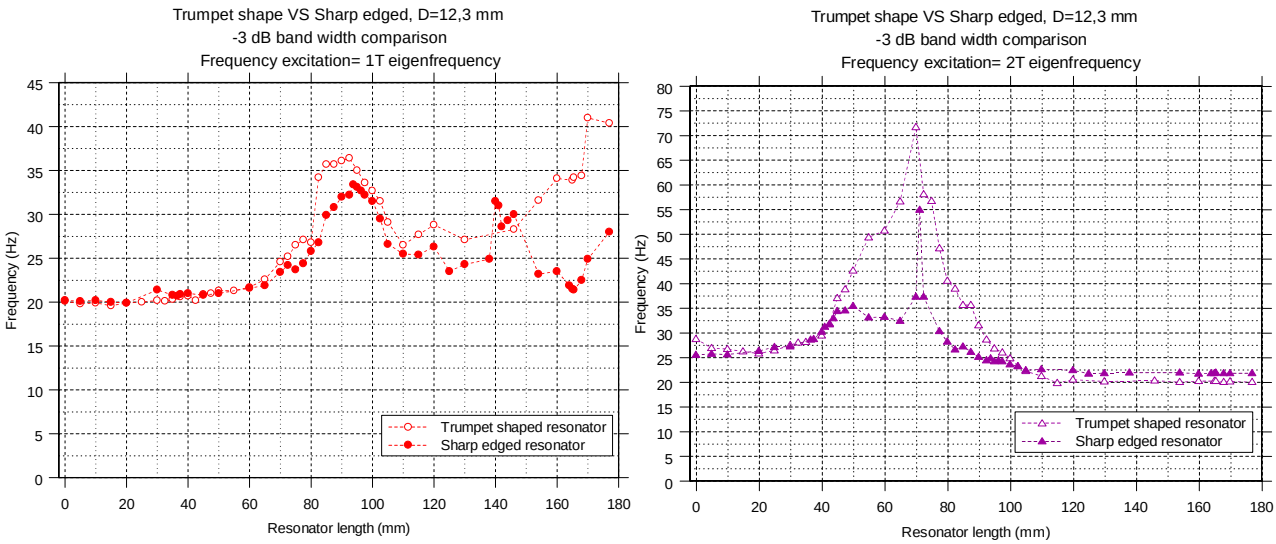


FIGURE 13: Measured FWHM values for the 1T (left) and 2T (right) modes; Chamber No. 1; Trumpet shaped (empty symbols) and sharp edged resonators (solid symbols), D = 12.3 mm

Surprisingly, the experiments with trumpet-shaped quarter wave tube are leading to higher acoustical damping in comparison to sharp edged ones. This experimental finding is in contrast to the expectation that velocity fluctuation at the inlet of the resonator is a key process for acoustical damping.

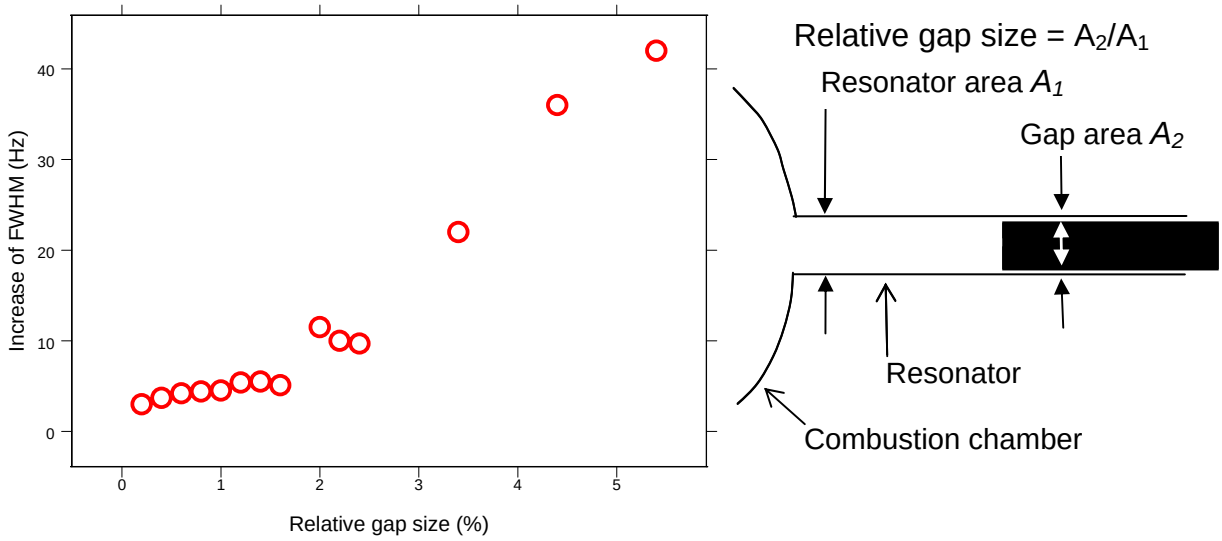


FIGURE 14: Increase of the 3-dB-width VERSUS gap size at the closed end of the resonator for non-dimensional resonator length of L / R = 0.85, $f_{excitation} = f_{1T}$
Chamber No. 1, Sharp edged resonator, D = 10 mm.

A tunable resonator has always an infinitesimal gap between the tube and the closing piston (see figure 14). However, even a very small gap at the closed end of a quarter wave resonator produces a strong increase of the acoustical damping, as can be seen in figure 14. At ordinate = abscissa = 0 the FWHM of the chamber without resonator equals 18 Hz. For the resonator length of L = 85 mm and the relative gap size of 0.2 %, the FWHM amounts to 21.5 Hz, thus the increase equals 21.5 – 18 = 3.5 Hz. While increasing the relative gap size, the increase of the FWHM grows steadily. A relative gap size of about 1.5 % leads to a doubling of the FWHM-increase compared to a hermetically closed end of the resonator. A relative gap size of about 4 % leads to an increase of the damping gain by a factor of 10. Possible implementations of this effect to oppress combustion oscillation of rocket engines are described in a patent application [3]

## 6 – Optimizing the resonator length for one coupled quarter wave cavity

The common way to determine the optimal resonator length is the evaluation of the so-called transfer-function. An important experimental finding in this study is the observation that for the resonator length leading to the highest obliteration of a given cylindrical eigenmode, the eigenmodes of the coupled system closest to the unwanted cylindrical resonance show a strong symmetry according amplitude, damping and intensity. Figure 15 shows examples for some particularities of the acoustical properties when the resonator length is optimized to suppress the first tangential eigenmode of the combustion chamber. The optimized length of $L$ = 85 mm is marked by a dash-line. In figure 10, the same length is marked, too. In figure 10, this is the length when the hyperbola of the lambda-quarter-tube frequency crosses the 1T cylindrical frequency of 1003 Hz. At this frequency, the right hand sides of the equations (2) and (3) are equal, thus equation (6) is true.

$$\frac{(2 \cdot l - 1) \cdot c}{4 \cdot L} = \frac{\alpha_{n,m} \cdot c}{2 \cdot \pi \cdot r} \qquad (6)$$

For $l$ = $m$ = $n$ = 1 and $r$ = 0.1m, thus for chamber No. 1, equation (6) is true at L = 85.3mm. For about the same resonator length, namely at $L$ = 84 mm, the FWHM for the excitation of both the 1T and the 2T eigen-modes is the same ($FWHM_{1T}$ =$FWHM_{2T}$ = 36 Hz). And for about the same length, at $L$ = 85 mm, the micro-phone voltage of the excitation of above eigenmodes is the same, too ($U_{1T}$ =$U_{2T}$). Further, at this resonator length, the pedestal intensity of both signals is the same, too.

When the hyperbola of the lambda-half-tube frequency crosses the 1T cylindrical frequency in figures 10 and 12, the right hand sides of the equations (1) and (3) equal, thus equation (7) is true.

$$\frac{l \cdot c}{2 \cdot L} = \frac{\alpha_{n,m} \cdot c}{2 \cdot \pi \cdot r} \tag{7}$$

For chamber No. 1 this is the case at the length of about 170 mm. At this resonator length, the 1T eigenfrequency is roughly $f_{1T} \approx 500$ Hz, thus $2 \cdot f_{1T} \approx f_{2T}$. For about this length, namely in the length range of $160 < L < 170$ mm, the 1T-FWHM-width for sharp-edged resonator has a minimum. For trumpet shaped resonator, however, the 3-dB-width increases steadily with the resonator length in the same length range, as can be observed in figure 13, left. The disagreement between the FWHM development for trumpet shaped and sharp edged resonators cannot be explained and needs further examination, in order to provide resonator design with optimized damping capacity.

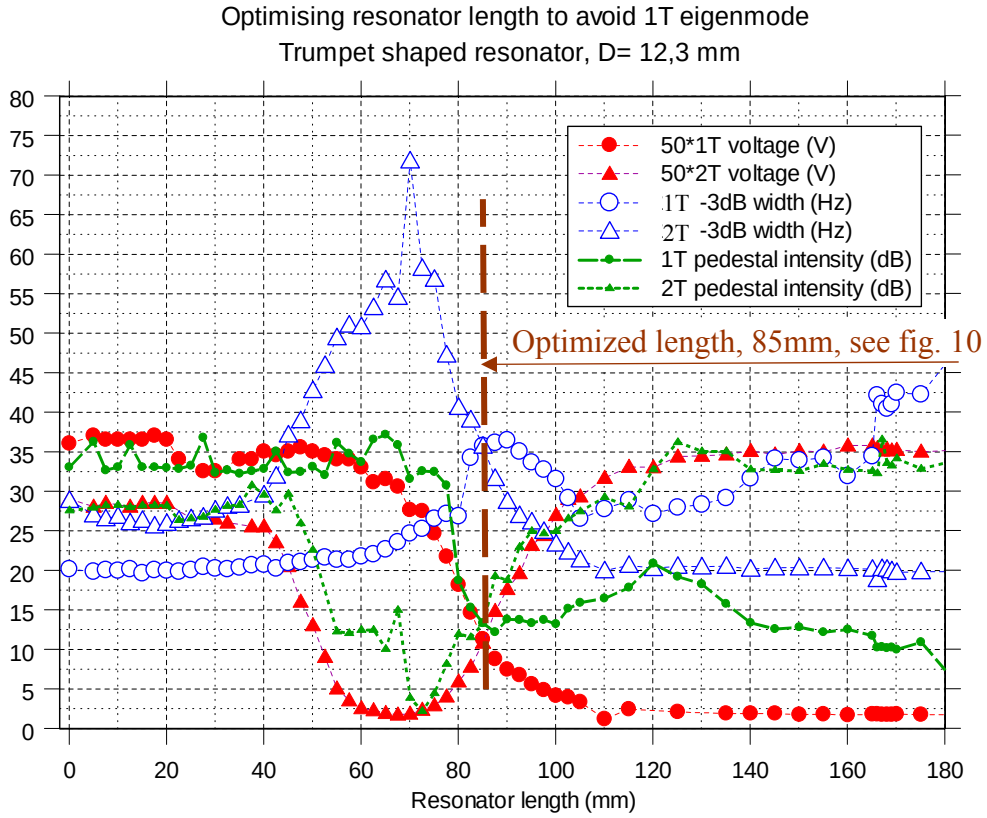


FIGURE 15: FWHM width, microphone voltage and pedestal intensity at optimized resonator length to suppress the 1T mode oscillation; Chamber No. 1, Sharp edged resonator, D = 12.3 mm.

Equation (6) permits a quick determination of the optimized resonator length for one quarter wave cavity coupled to a cylindrical resonator. Since the length of the quarter wave tube us not identical to the so called effective tube length, a fine tuning of the resonator is required to achieve best damping. The equality of the acoustical properties of the 1T and 2T modes at the optimized length, as shown in figure 15, leads to symmetry of the frequency distribution of above modes, too. Taking this symmetry has enabled the development of a quick and very effective measuring procedure leading to a patent application [4].

## 7 – Conclusion and outlook

In order to highlight the acoustical behavior of the more important tangential modes of combustion instabilities, the presented experiments were carried out on cylindrical chambers with low axial length. For studying nonlinearity of acoustical excitation, cylindrical chambers without resonator and coupled with one resonator were tested. The experiments certify that for cylindrical chambers without resonator, energy from eigenmodes with high eigenfrequencies emerge into modes in the lower frequency range. For coupled cylinder-resonator systems, the energy of excitation emerges from eigenfrequencies close to satisfy equation (6) into

eigenfrequencies close to satisfy equation (7). The experiments exposed symmetries according the acoustical properties of the 1T and 2T modes for λ/4-tubes having optimized resonator length. The detection of the symmetry led to a procedure for optimizing the resonator length described in a patent application [4]. The investigation of the effect of an infinitesimal gap at the closed end of a resonator led to another patent application for the increase of acoustical damping of combustion chambers [3].

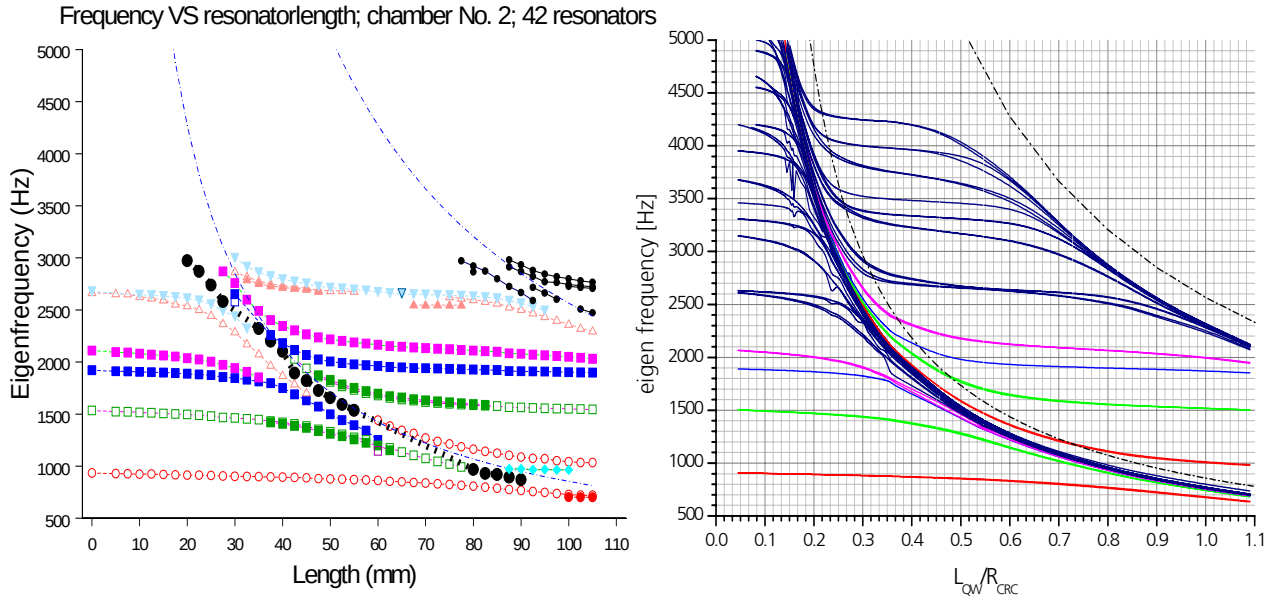


FIGURE 16: Influence of a cavity ring on the eigenfrequency; Chamber No. 2, 42 Resonators; Left: experiment; Right: calculation using FlexPDE®

Presently, the focus of investigation regards the effect of a cavity ring on the acoustical properties. The experiments are accompanied by calculations using FlexPDE® common software, a finite element method for the solution of partial differential equations. A comparison of calculation and experiment for a cavity ring of a steam generator is presented in figure 16. The steam generator to be examined has a geometry configuration close to rocket engines. For experiment and calculation plotted in figure 16, the axial length is 44 mm. The ongoing examination includes, however, the axial length of the combustion chamber with a cavity ring containing 42 quarter wave resonators. The goal of the investigation of the cavity ring as damping equipment is to proof if and how much the optimized shape and length of one quarter wave tube coupled to a cylindrical resonator are identical to those of a cavity ring.

## 8 – References

[1] B. Knapp, M. Oschwald, S. Anders: Untersuchung der tangentialen Moden von hochfrequenten Verbrennungsinstabilitäten in Raketenbrennkammern; DGLR – Jahrestagung 2005, Paper No. 189, September 2005

[2] G. Searby and F. Cheuret: Laboratory scale investigations of acoustic instability in a cylindrical combustion chamber, Proceedings of 7th French-German Colloquium on Research in Liquid Rocket Propulsion, 17-18 September 2002, Orléans France. CDROM,
Editors I. Gökalp and C. Chauveau, LCSR Orléans.

[3] Z. Faragó: Resonator device to adjust acoustical properties of a combustion chamber; Patent application, German Patent Office, German Aerospace Establishment (applicant), Application No. 10 2005 050 029.3, October 2005

[4] Z. Faragó: Procedure to adjust acoustical properties of a combustion chamber; Patent application, German Patent Office, German Aerospace Establishment (applicant), Application No. 10 2005 035 085.2, July 2005